Available online at www.sciencedirect.com

jmr&t Journal of Materials Research and Technology

journal homepage: www.elsevier.com/locate/jmrt

Original Article

Piezocatalytic dye degradation using Bi_2O_3-ZnO-B_2O_3 glass-nanocomposites

Chirag Porwal [a], *Moolchand Sharma* [a], *Rahul Vaish* [a], *Vishal Singh Chauhan* [a], *Samia ben Ahmed* [b], *Wonseop Hwang* [c], *Heyong Kwang Benno Park* [c], *Tae Hyun Sung* [c], *Anuruddh Kumar* [d,*]

[a] *School of Mechanical and Materials Engineering, Indian Institute of Technology Mandi, Mandi, Himachal Pradesh 175005, India*

[b] *Department of Chemistry, College of Sciences, King Khalid University, P.O. Box 9004, Abha, Saudi Arabia*

[c] *Department of Electrical Engineering, Hanyang University, Seoul 04763, South Korea*

[d] *Center for Creative Convergence Education, Hanyang University, Seoul 04763, South Korea*

ARTICLE INFO

Article history:
Received 31 August 2022
Accepted 10 October 2022
Available online 14 October 2022

Keywords:
Glasses
Nanocrystals
Piezocatalysis
Crystallization
Phytotoxicity

ABSTRACT

The presence of toxic compounds in waste leads to unfavorable hazardous properties, there is an urgent urge for the remediation of environmental contamination. This work focuses on the removal of organic pollutants from the water. Piezocatalytic properties of transparent glass nanocomposites of $Bi_2ZnB_2O_7$ (BBZO) were studied for water-cleaning application. Melt quenching followed by heat treatment of fabricated glass-nanocomposites were able to degrade different organic dyes. To study the microstructure of the samples under consideration, X-ray diffraction (XRD) and high-resolution transmission electron microscopy (HR-TEM) were performed. To get the elemental composition of the glass nanocomposite samples, XPS (X-ray photoelectron spectroscopy) was utilized. Methylene blue (MB) dye was used as a model dye for degradation, and it is found that heat-treated glass nanocomposite sample at 475 °C for 1 h (HT/475 °C/1hr) gives maximum dye degradation of 78% under 240 min of ultrasonication with a degradation rate of 0.0065min^{-1}. Furthermore, an obtained by-product from degraded dye was used to experiment to study phytotoxicity assessment using brown gram seeds and it has been found that treated water with BBZO HT/475 °C/1hr sample gives less phytotoxicity of water (Germination Index is found to be 88%).

1. Introduction

Nowadays, the numerous pollutants found in the water, soil, and air provide a persistent threat to the natural environment [1]. To create a comfortable environment, many enterprises are set up to satisfy human wants, which results in a significant volume of biological waste that needs to be managed. This waste contains poisonous substances, and because of its

* Corresponding author.
E-mail address: anuruddh07@hanyang.ac.kr (A. Kumar).

https://doi.org/10.1016/j.jmrt.2022.10.041

risky characteristics, they create an ecosystem that could harm human health [2]. There is a pressing need to address environmental contamination since fresh water, clean air, and healthy soil are essential for maintaining life on earth. The goal of this work is to purge the water of organic pollutants. Research on wastewater remediation is still ongoing, and wastewater from businesses like textile and pharmaceutical contains organic waste in the form of dyes. The development of photocatalysis using semiconductors, which has been used for pollutant decomposition by the generation of reactive oxygen species and their recombination into dye molecules in the presence of ultraviolet and visible light sources to degrade and clean water is still in development [3–5].

Borate-based crystals are a known family of materials in optics. It is because of associated nonlinear optical properties, fluorescence, laser hosts, optical filters, X-ray and γ-ray absorbers, photonic devices, and other potential applications [6]. These crystals include $Li_2B_4O_7$, $BiBaBO_4$, Li_3BO_3, etc. [7,8]. Above mentioned crystals are non-centrosymmetric and demonstrate nonlinear optical properties. As crystals always have a higher cost and longer manufacturing process, researchers have been exploring borate-based glass-ceramics as a possible substitution for borate-based crystals [9,10]. Borate-based glass ceramics can easily be fabricated by the conventional melt quenching technique as borates are good glass former and have a moderate melting point. There are significant articles that are published on transparent borate-based glass-ceramics in the domain of ferroelectric glass-ceramics. Two decades from 1990 to 2010 witnessed borate-based ferroelectric glass ceramics [11–15]. These glass-ceramics have also shown potential in electrical energy storage devices due to higher electrical breakdown strength as no porosity exists in glass-ceramics fabricated from the melt quenching method [16–20]. Some of these glass-ceramics have also demonstrated piezoelectric properties in the case of oriented crystallization. One of the very important features of glass-ceramic is controlled microstructure (crystallization) for desired physical properties.

In order further explore any novel application of these glass ceramics, catalysis for water treatment and self-cleaning point of view could be promising. A review article has been published for photocatalyst glass-ceramics as well as possibilities of borate for catalytic applications [9].

Piezocatalysis is another type of catalysis where a piezoelectric semiconductor can act as a catalyst [21]. There are many articles published in piezocatalysis using polycrystalline ceramics [22–24]. A ferroelectric material can demonstrate piezoelectric properties only after electrical poling. Ferroelectric ceramics have shown effective piezocatalytic performance in poled samples [25,26]. It is already established that catalyst in powder form is difficult to recover and reuse. Utilizing poled ceramic in pellet form was able to overcome the drawback of powder as a catalyst, but its applicability is limited by the need for a high power source for poling. Therefore in the finding of potential catalyst for water remediation, Glass-nanocomposite, an emerging area need to be investigated. Non-centrosymmetric glass-nanocrystals can exhibit piezocatalysis even without poling, in the case of nano-crystals single domain material [27–29]. As the catalysis process is associated with local piezoelectric properties, every crystal embedded in the glass nanocomposite can act as a piezoelectric crystal for catalytic applications [30].

From the above-mentioned discussion, catalytic glass nanocomposite can be a game changer and open a new direction for glass nanocomposite applications. To understand, piezocatalysis in glass nanocomposites. $Bi_2ZnB_2O_7$ (BBZO) is selected here. BBZO is a polar material and has significant borate [21–26]. Borate is important for glass-ceramic formation. In this study glass-ceramics for BBZO compositions were fabricated and investigated for piezocatalysis applications.

2. Experimental

For the synthesis of $Bi_2ZnB_2O_7$ (BBZO) transparent glass nanocomposites, the conventional melt quench technique was used. Initially, ZnO, Bi_2O_3, and H_3BO_3 reagents of high grade (purity >99%, Fisher Scientific) were used according to their stoichiometric ratio for the fabrication of glass under consideration. All the initial precursor powders were mixed properly in the mortal pestal for 30 min to get a homogenous mixture, then obtained mixture was transferred to a platinum crucible. The crucible with the prepared powder is then placed in a Nabertherm furnace set to 1000 °C for 5 min to melt the powder. The melt was then poured onto a hot stainless-steel plate at 350 °C and pressed with another hot plate at the same temperature to quench the desired glass of $Bi_2ZnB_2O_7$ chemical compositions. To ensure their strength and minimize thermal stresses, the produced glass plates were annealed at 350 °C for 5 h. After quenching, the transparent yellow BBZO glass plate is heated to a different temperature to achieve crystallization of the samples following the previously reported Differential scanning calorimetry (DSC) data

Table 1 – Comparison of catalytic activity of ferroelectric materials to present study.

Catalyst	Catalytic phenomenon	Targeted pollutant (concentration)	Power source specification	Rate constant (k)	Reference
$LiNbO_3$ glass -ceramics	Piezocatalysis	Methylene Blue (5 mg/L)	40 kHz, 70W ultrasonicator	0.01281 min^{-1}	[35]
$BaTiO_3$ nanowires	Piezocatalysis	Methyl orange (5 mg/L)	40 kHz, 80W ultrasonicator	0.015 min^{-1}	[36]
$BaTiO_3$ nanoparticles	Piezocatalysis	Methyl orange (5 mg/L)	40 kHz, 80W ultrasonicator	0.019 min^{-1}	[37]
$Zn_4B_6O_{13}$	Photocatalysis	TC solution (1.6 mg/mL)	UV light	0.0067 min^{-1}	[38]
$InBO_3$	Photocatalysis	4-CP (0.325 mg/mL)	$\lambda > 30$ nm, UV light	0.043 min^{-1}	[39]
$Bi_2ZnB_2O_7$	Piezocatalysis	Methylene Blue (5 mg/L)	40 kHz, 150W ultrasonicator	0.0065 min^{-1}	Present Study

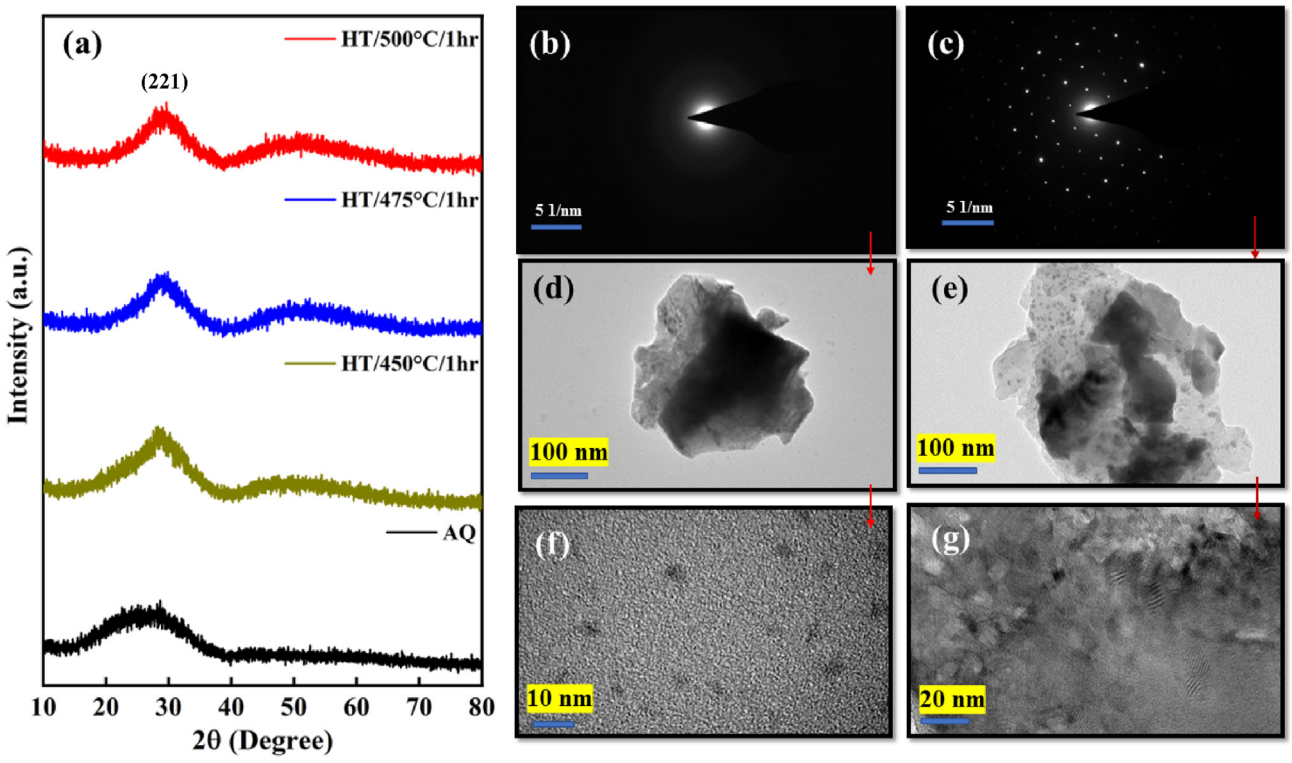

Fig. 1 – (a) XRD plots of AQ and heat-treated samples of BBZO glass at 450 °C, 475 °C, and 500 °C for 1 h, (b) and (c) are the diffraction pattern obtained with TEM, Obtained TEM images of AQ and heat treated at 475 °C for 1-h BBZO glass samples are (d), (f) and (e), (g) at respective scale.

[31]. To analyze crystal structure and phase purity, the produced glass nanocomposites of BBZO were evaluated using the X-ray diffraction (XRD) technique with a powder diffractometer from Rigaku (Japan) based on a Cu Kα rotating anode of 9 kW. Scan rates of 2°/minutes were used for XRD in the 2θ range of 10°–80°. To study the nature of the glass nanocomposites, High-Resolution Transmission Electron Microscopy (HR-TEM) was also utilized. Imaging of all the samples under consideration was done by HR-TEM of FEI Company, USA (model: FP 5022/22-Tecnai G2 20 S-TWIN). A Nexsa X-ray photoemission spectrophotometer using an Al-Kα source was used to conduct X-ray photoemission spectroscopy (XPS) to validate the existence of elemental states in the synthesized BBZO glass nanocomposites. The obtained binding energy was calibrated using the 284.8 eV C1s peak. A Shimadzu (UV-2600) UV-visible spectrophotometer was also used to record all of the catalytic degradation rates. Piezocatalytic dye degradation was carried out using prepared samples of BBZO glass nanocomposites (AQ, HT/450 °C/1hr, HT/475 °C/1hr, and HT/500 °C/1hr). All the initial degradation experiments were done with Methylene blue as a model dye. A 5 mg/L concentration of MB was initially present in a 10 mL solution. Samples of BBZO glass nanocomposites with a surface area of 140 mm^2 were dipped in a 10 mL dye solution. Before beginning catalytic studies, adsorption equilibrium was to be reached and for that, the glass nanocomposite samples containing dye solution were left in the dark for 24 h. Following this, ultrasonication was performed using a 150 W ultrasonicator functioning at a 40 kHz frequency. Every 30 min, the ultrasonic medium (water) was changed to avoid a temperature increase that would cause thermocatalytic dye degradation. A 1000 μL proportion of the solution was examined and then added back to the main solution at specified intervals of 30 min due to the possibility that high temperatures could cause water to evaporate. Monitoring the fluctuations in dye concentration allowed for the determination of the shift in a relative position of the MB dye absorption peak in a UV-visible spectrophotometer. Equation (1) was used to assess the dye degradation obtained (in terms of %). The pseudo-first-order rate constant was examined using the following equations (2) and (3) to determine the reaction kinetics [32].

$$D\% = \left(\frac{A_0 - A}{A_0}\right) \times 100 = \left(\frac{C_0 - C}{C_0}\right) \times 100 \quad (1)$$

$$C = C_0 e^{-kt} \quad (2)$$

$$In\,[C / C_0] = kt \quad (3)$$

Here, A_0 and C_0 stand for the pollutant solution's original absorbance and concentration, whereas A and C stand for the pollutant solution's vague absorbance and concentration, respectively. D % calculates the percentage of pollutant degradation. The reaction time is expressed by t, whereas k specifies the pseudo-first-order rate constant. According to the methodology for the germination test, brown gram seeds were properly washed multiple times with distilled water before the experiment to achieve surface sterilization. Then, each pair of four replicates of five seeds was given 4

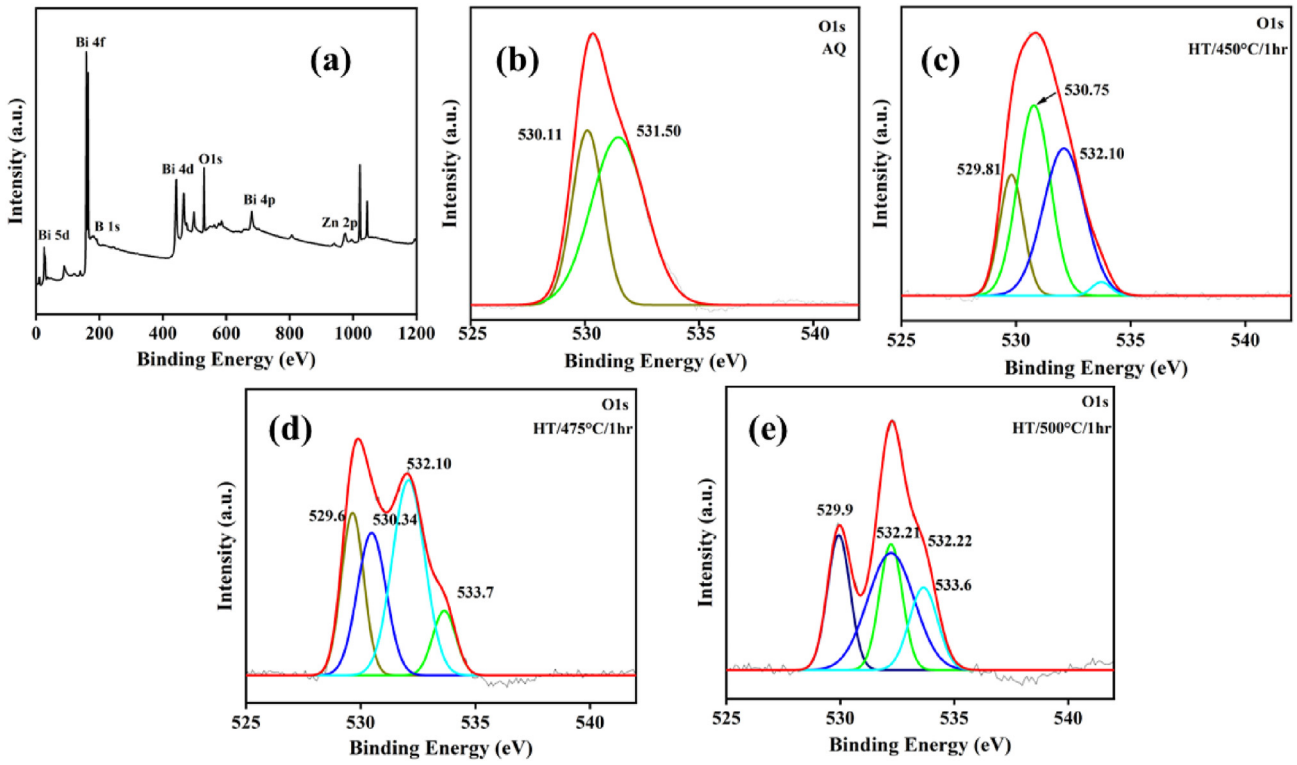

Fig. 2 – (a) XPS survey with (b)–(e) O1s plots of AQ, heat-treated at 450 °C, 475 °C, and 500 °C for 1-h BBZO glass samples.

treatments (distilled water, treated 5 mg/L MB, untreated 5 mg/L MB, and 100 mg/L MB dye) in four 10 mL glass vials. As a control, distilled water was used; 1 mL was added on the first day, and 0.5 mL was added every day after that. For seven days, the glass vials were kept in the chamber at a constant room temperature. When the cotyledons of the seed had expanded to a length of more than 2 mm, the seeds began to sprout. Radicle length, plumule length, and germination percent were used to calculate the germination index (GI), which was then calculated using the following equation (4) [33].

$$GI\,(\%) = \frac{\text{Seed germination}\,(\%) \times \text{root length of treatment}}{\text{Seed germination}\,(\%) \times \text{root length of control}} \times 100 \quad (4)$$

3. Results and discussion

X-ray diffraction (XRD) measurements were performed on all the fabricated BBZO glass and glass nanocomposite samples (AQ and heat-treated) and are shown in Fig. 1(a). As seen in the obtained XRD plots, AQ glass substantiates the amorphous nature along with heat-treated samples. In addition, HT/450 °C/1hr, HT/475 °C/1hr, and HT/500 °C/1hr glass nanocomposites samples also do not exhibit any clear peaks for the crystallographic planes in obtained pattern. As noted from all the attained patterns, the sharpening of the peak is occurring from AQ to HT/500 °C/1hr BBZO glass nanocomposites sample giving rise to (221) plane of $Bi_2B_2ZnO_7$ (ICSD file no: 152281) and hence, giving rise to an idea about the advancement of nanocrystals in the glass matrix. Generally, XRD is considered a bulk technique, with the purpose to investigate the possibilities concerning the formation of nanocrystals, high-resolution transmission electron microscope (HR-TEM) imaging is conducted for AQ and HT/475 °C/1hr glass nanocomposite samples. The obtained selected area electron diffraction (SAED) pattern and the image are shown in Fig. 1(b)-(g). Fig. 1(b) is the attained SAED pattern for the AQ glass sample and, it is noted that there is no diffraction present in it, revealing its amorphous nature. The captured images presented in Fig. 1(d) and (f) show that there are no/few crystals present in the AQ glass sample. Fig. 1(c) is the observed SAED pattern for the heat-treated BBZO glass nanocomposite sample at 475 °C for 1 h, which confirms the presence of nanocrystals in the glass matrix. The same can be validated by the images shown in Fig. 1(e) and (g).

The surface chemical state and chemical constitution of the BBZO glass nanocomposite samples were investigated using X-ray photoelectron spectroscopy (XPS). The acquired survey spectra are shown in Fig. 2(a) which is illustrating the elemental existence in the parent glass of BBZO. Bi 4p, Bi 4f, Bi 4d, Bi 5d, B 1s, O 1s, Zn 2p, and C 1s of the currently present elements in BBZO are highlighted in the wide range XPS survey showing the presence of elemental states at different binding energies. The change in the oxygen peak positions was observed for the AQ, HT/450 °C/1hr, HT/475 °C/1hr, and HT/500 °C/1hr glass nanocomposite samples are shown in Fig. 2(b–e). For the AQ glass sample, the spin-orbital states were found to be at 530.11 eV and 531.50 eV binding energy in the O1s plot. As the heat treatment to the samples takes place, a change in the peak position and splitting of the peak in

oxygen spectra can be observed. The presence of oxygen in the sample can be quantified in the terms of bridging sites (BO) and non-bridging sites (NBO). The possible reason for the peak shift from AQ to heat-treated samples may be the addition of network modifiers such as Zn. The crystallization of glass samples enables Zn to increase the NBO and decrease the BO in the crystal structure of the glass sample. Peaks at 530 ± 0.3 eV are due to the Zn-O and the rest are due to the adsorbed hydrocarbon from the environment [34].

Transmittance and absorbance spectra were collected for the AQ, HT/450 °C/1hr, HT/475 °C/1hr, and HT/500 °C/1hr BBZO glass nanocomposite samples with UV-vis spectroscopy in the range of 200–800 nm at room temperature and obtained plots are shown in Fig. 3. Fig. 3(a) shows the effect of heat treatment on the transparency of the samples under consideration and it is observed that the transparency reduces as the temperature of heat treatment increases. It is obvious that because of crystallization, transparency is reduced. Due to the presence of nanocrystals, the reduction in transparency is very less. The obtained absorbance spectra as shown in Fig. 3(b) indicates an increase in absorbance as the transparency of the sample is reduced. Interestingly, transparency was not decreased with heat treatment. It is due to the fact that the chemical composition of crystals and the amorphous matrix is very close and hence refractive index would be very similar. The scattering will also be minimal as these glasses have nanocrystals.

Piezocatalysis is used to eradicate contaminants from the organic dye (MB) using samples of BBZO glass nanocomposite ceramics. Fig. 4 represents the results of dye degradation using AQ, HT/450 °C/1hr, HT/475 °C/1hr, and HT/500 °C/1hr in comparison to control MB dye degradation. Fig. 4(a) illustrates how the peak intensity of the sample of HT/475 °C/1hr, which has the highest dye degradation among the samples under investigation, decreased during 240 min of piezocatalysis. The results show that the BBZO glass nanocomposite sample can degrade dye when introduced to ultrasonication. Fig. 4(b) demonstrates the samples under consideration capability as a catalytic material for dye degradation in the form of C/C_0 to time. Fig. 4(d) illustrates the acquired results for dye degradation of control MB dye, which were 12%, compared to AQ, HT/450 °C/1hr, HT/475 °C/1hr, and HT/500 °C/1hr BBZO glass nanocomposite samples, which were 38%, 74%, 78%, and 60%, respectively, after 240 min of ultrasonication. The specific surface area available in smaller crystals leads to more catalytic sites. Crystallization will be more pronounced and with increased heat treatment temperature and duration, catalytic activity may well diminish. A similar trend is observed here as depicted in Fig. 4(d). As discussed, the degradation follows first-order kinetics, Fig. 4(c) illustrates the calculated values of the rate constant (k) for the degradation process using several samples of BBZO glass nanocomposite samples. The obtained slopes for the control MB dye, AQ, HT/450 °C/1hr, HT/475 °C/1hr and HT/500 °C/1hr sample of BBZO are 0.0005min^{-1}, 0.0021min^{-1}, 0.0030min^{-1}, 0.0065min^{-1}, and 0.0058min^{-1}, respectively. HT/475 °C/1hr, which has the highest k value of 0.0065min^{-1} among the fabricated glass nanocomposite samples, has the highest dye-degrading capabilities. It is because the HT/475 °C/1hr sample has smaller crystals, which serve to enhance the specific surface area. Crystals grow as heat treatment temperatures and durations rise, while their specific surface areas decrease.

An indirect scavenger method was used to pinpoint the active species responsible for piezocatalytic activity. Together with the BBZO glass nanocomposite sample, three scavengers Ethylenediaminetetraacetic acid (EDTA), *p*-benzoquinone (PBQ), and Isopropyl alcohol (IPA), (10 mM each) were subsequently added to the test dye solution to acquire reactive oxygen species (ROS) like holes (h^+), superoxide ($\cdot O2^-$), and hydroxyl ($\cdot OH$). The primary active radical can be discovered because its capture results in the greatest reduction in catalytic performance. By trapping radicals, the observed order of dye degradation is BQ($\cdot O2$) > EDTA(h^+) > IPA($\cdot OH$). ($\cdot O2^-$) trapped by PBQ is the principal active species involved in dye degradation. For executing the experiments up to 5 cycles, the repeatability of the BBZO glass nanocomposite sample for piezocatalytic performance was evaluated, and the results have been plotted as shown in Fig. 5(c). There was no

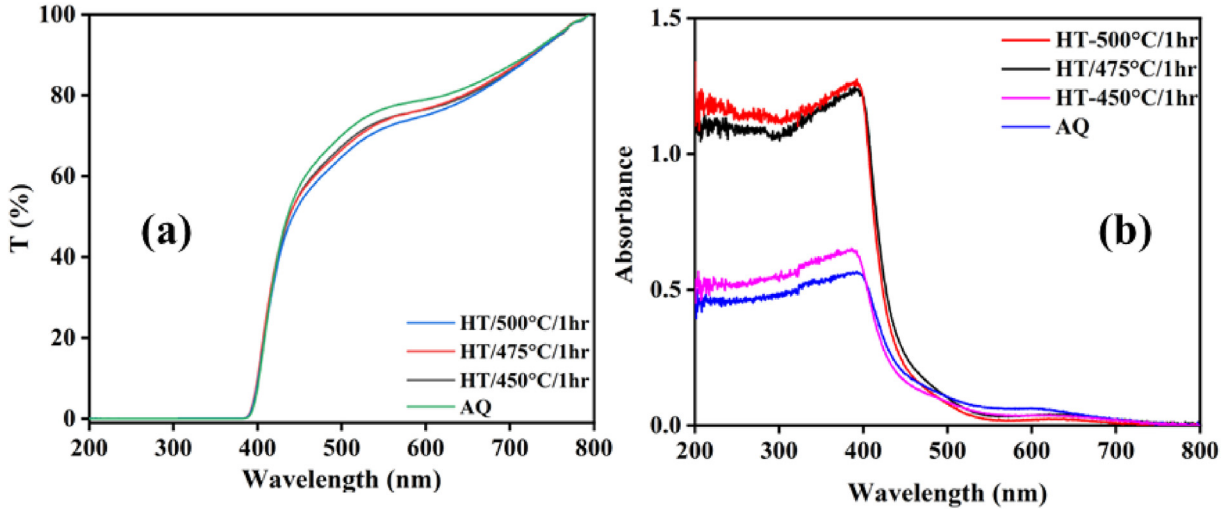

Fig. 3 – (a) Transmittance plot and (b) absorbance plot for AQ, heat-treated at 450 °C, 475 °C, and 500 °C for 1-hr BBZO glass samples.

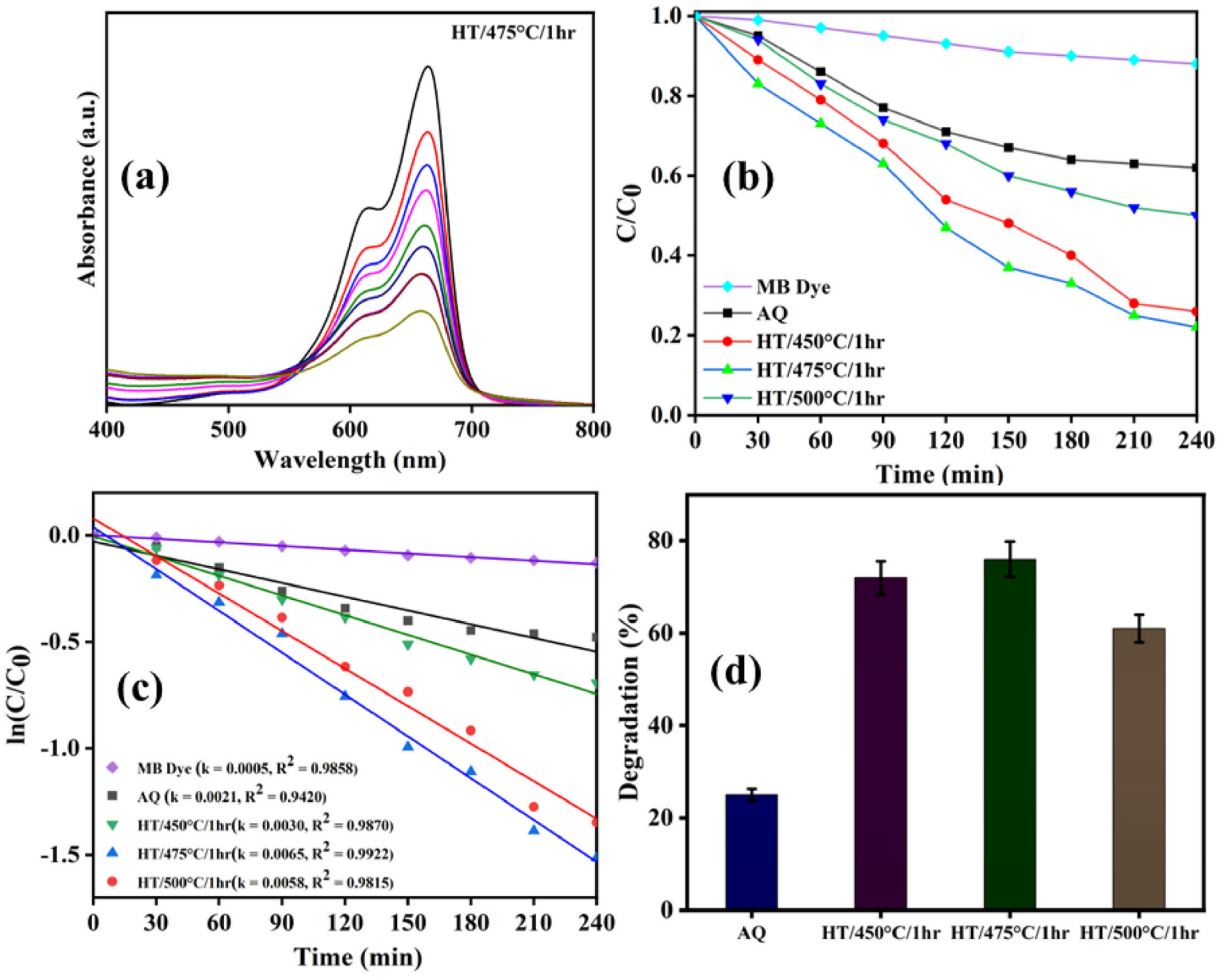

Fig. 4 – Piezocatalytic dye degradation: (a) Reduction in the peaks intensity while performing piezocatalysis with the heat-treated sample at 475 °C for 1 hr of BBZO glass (HT/475 °C/1hr). (b), (c) Results of piezocatalysis for all the fabricated samples as well as of pure MB dye in the terms of C/C_0 vs. time and ln C/C_0 vs. time for kinetic rate. (d) Results of dye degradation in the terms of percentage for all the samples under consideration.

discernible change, and BBZO is a potential candidate for reuse. Different kinds of dyes were investigated for piezocatalysis in addition to assessing the behaviour and capabilities of prepared BBZO glass nanocomposite samples. Methyl violet (MV) and Rhodamine B (RB) dyes, in addition to Methylene blue (MB), were investigated for 240 min of ultrasonication on a glass sample that had been heated for 1 h at 475 °C (HT/475 °C/1hr). Fig. 5(b) illustrates the outcomes of these experiments using varying dyes. As stated in Table 1, a comparison of such previously reported catalytic materials with the ongoing study has been done.

Crystalline non-centrosymmetric crystals possessing the ability to respond mechanically to an external electric field and vice versa fall under Piezoelectric. As a consequence of structural anisotropy, atomic displacement within the piezoelectric materials results in a mismatch between the cation and anion centers, which generates a dipole moment/polarization. There are two main theories to explain the piezo effect: the Energy Band Theory and the Theory of the Screening Charge Effect. A specific chemical reaction is mainly determined by the energy band levels (valence and conduction bands). Band bending of semiconductors normally occurs in the space–charge layer of the catalyst surface, which in turn induce an electric-potential gradient that boosts carrier separation and transfer. In energy band theory, the generated piezopotential initiates the reaction by modulating the band structure and managing the internal charge carrier flow to the surface of the catalyst surface. Screening charge effect, prioritize the roles of piezopotential along with associated surface-charged adsorbates from an external system. These adsorbed charges are called external screening charges. These charges from the external system participate in the redox reactions and not the internal charges from the material. In short, polarization generated in material induces an opposite charge near the surface of the catalyst. More importantly, the surface screening behaviour induced by polarization governs the piezocatalytic process. The magnitude of the piezopotential must fully satisfy the required redox level and determine the ability of the piezocatalyst to realize a specific chemical transformation [40].

The complete process flow of dye degradation via piezocatalysis using fabricated BBZO glass nanocomposite is shown

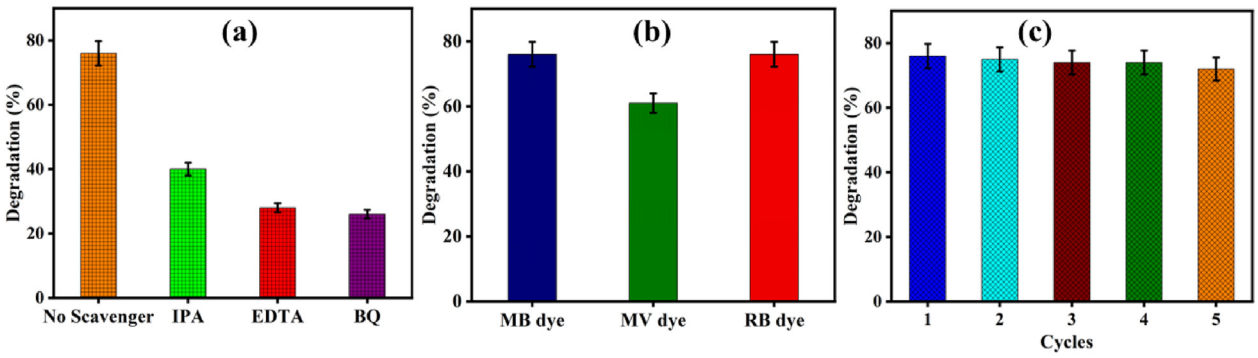

Fig. 5 – (a) Scavenger test for radical trapping, (b) degradation using different dyes, and (c) repeatability test.

with the help of a schematic in Fig. 6. To accomplish composition homogeneity, initial precursor powders were thoroughly pulverized in a mortar and pestle. Then, the composition was transferred to the platinum crucible. After that, to melt the prepared powder, the crucible containing it is placed in a furnace. The appropriate glass was then quenched by pouring the melted powder onto a hot stainless-steel plate at a temperature and pressing it with another hot plate of the same temperature. The obtained BBZO glass was then subjected to different heat treatments as per the experimental conditions and then piezocatalytic dye degradation was accomplished. To get rid of organic impurities from water, MB dye is used. Experiments incorporating the ultrasonication of water results in bubble formation, expansion, and ultimately collapse. The continual cycle of this bubble formation, expansion, and collapse results in high-temperature regions of roughly 5000K with a high-pressure wave of 10^8 Pa. At this high pressure and temperature, the bubble breaks down into radical species, interacting with the dye to contribute to the breakdown process of sonolysis (thermolysis) [41,42]. The obtained results show that, in comparison to heat-treated samples, self-dye degradation values are almost negligible. Without any samples, ultrasonication caused the dye to degrade by thermolysis at a rate of 12% in 240 min. However, the BBZO glass nanocomposite samples that were employed helped to degrade the dye by piezocatalysis. The BBZO glass nanocomposite samples that produce piezoelectricity during ultrasonication separate charges by electrochemistry, which causes the dye to degrade through redox processes. Piezo sensitization is another potential method of dye degradation. The excited state of the surface-complexed dye molecules is captured onto the surface of the BBZO glass-nanocomposite sample by the positive charge produced by mechanical vibrations. The degradation of the dye is facilitated by this surface redox process. The following is an explanation of a potential piezocatalytic dye degradation mechanism [43]:

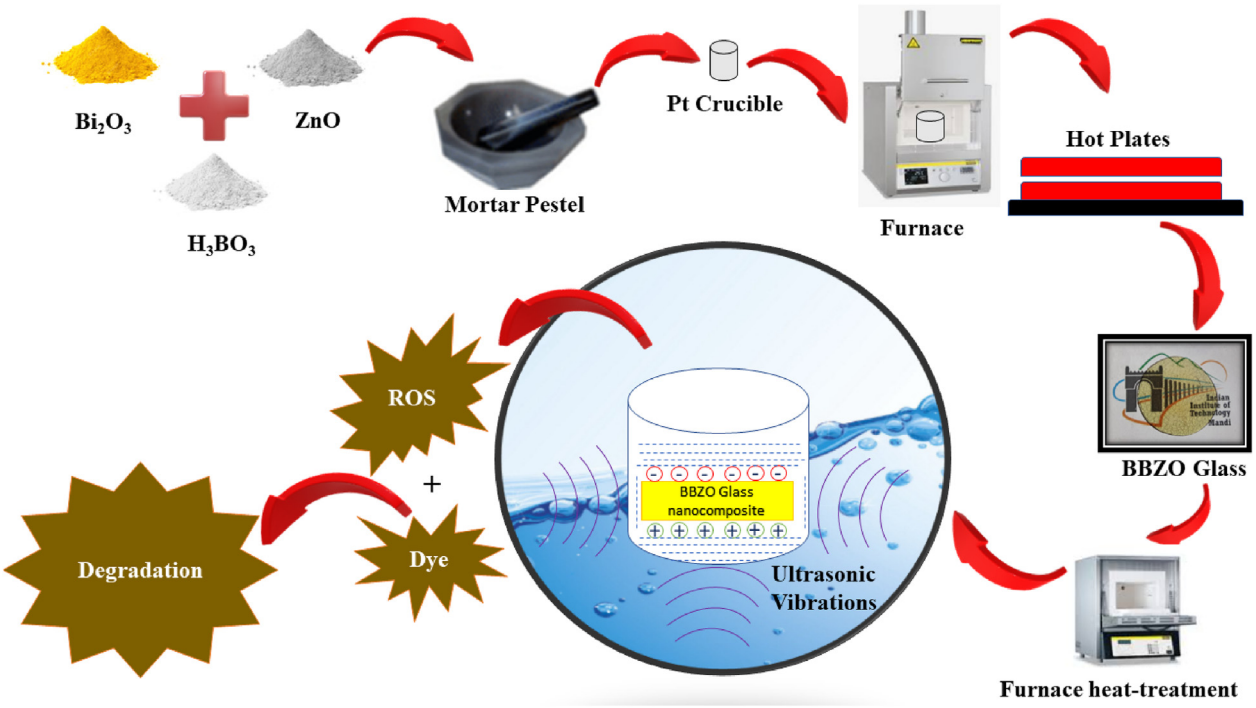

Fig. 6 – Schematic layout for synthesis and piezocatalytic dye degradation using BBZO glass nanocomposites.

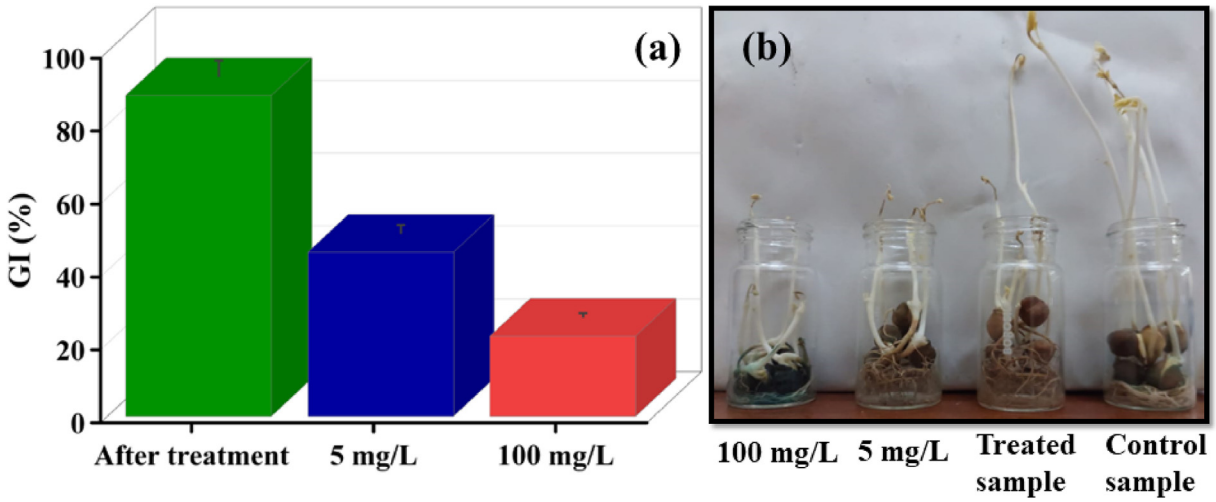

Fig. 7 – (a) Germination index of MB dye (1) after piezocatalysis, (2) before piezocatalysis, (3) 100 mg/L dye solution (DI is used as control), (b) demonstration of treated MB dye water for growing brown gram seeds.

$$BBZO\ glass-ceramics\ \ sample\ \rightarrow BBZO\ glass-ceramics\ sample\ (e^{-}+h^{+}) \quad (5)$$

$$e^{-}+O_2 \rightarrow \ \bullet O_2^{-} \quad (6)$$

$$h^{+}+OH^{-} \rightarrow \ \bullet OH \quad (7)$$

$$\bullet O_2^{-}+Dye \rightarrow Degradation \quad (8)$$

$$\bullet OH+Dye \rightarrow Degradation \quad (9)$$

An electric field is produced when the crystallite of BBZO glass nanocomposite samples is strained by ultrasonic vibrations. This causes polar surface generation as one negative and one positive due to a localized electric field. The influence of this localized electric field promotes the generation of free radicals by causing segregated charges in the BBZO crystallites to migrate toward the surfaces (e^{-} to the positive surface and h^{+} to the negative surface, respectively). A free electron will be captured on the positive surface, where it will interact with the hydroxyl ion to form the radical hydroxyl, and the dissolved oxygen will have been reduced to produce superoxide anions. These generated •O2^{-}, •OH act as strong oxidants, which will attack dye molecules giving degradation of dye as result.

Water sources used for irrigation include untreated textile industry wastewater because it is related to ecosystem security, this practice of discharging effluents directly into water bodies is tremendously damaging to the environment. Both directly and indirectly, irrigation water affects soil fertility. Numerous byproducts are produced during the biodegradation of wastewater. Therefore, it is crucial to research how hazardous these metabolites are to plants. Frequently eaten sprouts of brown gram seeds have been used to check the sensitivity towards the byproducts of MB dye. % Germination was evident in the control sample, the germination index for all three samples is shown in Fig. 7(a) and, brown gram seeds germination data after 7 days are shown in Fig. 7(b). At IIT Mandi in India, all seed germination studies were conducted at a temperature of 25 °C. The lengthening of the seeds will be inversely correlated with the toxicity of the water used for seed germination. Consequently, the seed that is cultivated using treated water will be a non-toxic indication. Phytotoxicity is analyzed based on its GI values, GI<50%, GI>80%, and 50%<GI<80% for high phytotoxicity, low or absence phytotoxicity, and medium phytotoxicity. As shown in the figure, it has been observed that GI values of 5 mg/L and 100 mg/L are 45% and 22% whereas treated water GI is 88% which falls in the category of less phytotoxicity. Varying several parameters like concentration of MB dye, increase in catalyst amount or different catalytic processes will hopefully enhance the GI value.

4. Conclusions

BBZO ($Bi_2ZnB_2O_7$) glass nanocomposites were fabricated using the conventional melt quenching technique and optimum selected heat treatment was done to get desired crystallization of the glass samples. XRD (X-ray diffraction) was carried out on AQ, HT/450 °C/1hr, HT/475 °C/1hr, and HT/500 °C/1hr glass nanocomposite samples, which shows amorphous nature with a converging peak leading to an idea of the development of nanocrystals. To confirm the crystalline nature of the prepared glass nanocomposites, HR-TEM (High-resolution transmission electron microscopy) was done. The observed diffraction pattern with high-resolution images of the samples, confirms the presence of nanocrystals in it. To get the elemental composition of the glass sample under consideration, XPS (X-ray photoelectron microscopy) was utilized and the obtained results confirm the presence of all the constituents with their orbital states in the BBZO glass nanocomposite samples. Piezocatalysis technique was used to get degradation of dye with MB dye as a model dye and it is found that heat-treated glass nanocomposite sample at 475 °C for 1 h

(HT/475 °C/1hr) gives maximum dye degradation of 78% under 240 min of ultrasonication with a degradation rate of 0.0065min^{-1}. To confirm the reliability and capabilities of prepared glass samples, different dyes were used and experiments were repeated five times. Furthermore, an obtained by-product from degraded dye was used for phytotoxicity assessment using brown gram seeds and it has been found that treated water with BBZO HT/475 °C/1hr sample has reduced phytotoxicity of water (GI = 88%).

Declaration of Competing Interest

The authors declare that they have no known competing financial interests or personal relationships that could have appeared to influence the work reported in this paper.

Acknowledgments

This work was supported by the Korea Institute of Energy Technology Evaluation and Planning (KETEP) and the Ministry of Trade, Industry & Energy (MOTIE) of the Republic of Korea (No. 2018201010636 A and 20204010600090). The authors extend their appreciation to the Deanship of Scientific Research at King Khalid University, Saudi Arabia for funding this work through Large Research Groups Program under grant number L.R.G.P2/171/43.

REFERENCES

[1] Park S, Labys W. Industrial development and environmental degradation. BOOKS; 1998.
[2] Mudu P, Terracini B, Martuzzi M. Human health in areas with industrial contamination. 2014.
[3] Qian W, Zhao K, Zhang D, Bowen CR, Wang Y, Yang Y. Piezoelectric material-polymer composite porous foam for efficient dye degradation via the piezo-catalytic effect. ACS Publ 2019;11:27862–9. https://doi.org/10.1021/acsami.9b07857.
[4] Kabra K. Treatment of hazardous organic and inorganic compounds through aqueous-phase photocatalysis: a review. Ind Eng Chem Res 2004;43:7683–96. https://doi.org/10.1021/ie0498551.
[5] Hayati B, Mahmoodi NM, Maleki A. Dendrimer-titania nanocomposite: synthesis and dye-removal capacity. Res Chem Intermed 2015;41:3743–57. https://doi.org/10.1007/S11164-013-1486-4.
[6] Gautam Chandkiram, Avadhesh Kumar Yadav AKS. A review on infrared spectroscopy of borate glasses with effects of different additives. Int Sch Res Notices 2012. https://doi.org/10.5402/2012/428497.
[7] Reshak AH, Kityk IV, Auluck S. Energy band structure and density of states for BaBiBO4 nonlinear optical crystal. J Alloys Compd 2008;460:99–102. https://doi.org/10.1016/j.jallcom.2007.06.070.
[8] Ranjeh M, Beshkar F, Engineering MS-N. Sol-gel synthesis of novel Li-based boron oxides nanocomposite for photodegradation of azo-dye pollutant under UV light irradiation. Compos B Eng 2019;172:33–40. https://doi.org/10.1016/J.COMPOSITESB.2019.05.085.
[9] Yang J, Sun X. Borate particulate photocatalysts for photocatalytic applications: a review. Int J Hydrogen Energy 2022. https://doi.org/10.1016/J.IJHYDENE.2022.05.305.
[10] Bengisu M. Borate glasses for scientific and industrial applications: a review. J Mater Sci 2016;51:2199–242. https://doi.org/10.1007/S10853-015-9537-4.
[11] Wu J, Qin N, Yuan B, Lin E, Bao D. Enhanced pyroelectric catalysis of BaTiO 3 nanowires for utilizing waste heat in pollution treatment. 2018. https://doi.org/10.1021/acsami.8b11158.
[12] Kurihara T, Okutomi H, Miseki Y, Kato H, Kudo A. Highly efficient water splitting over K 3Ta 3B 2O 12 photocatalyst without loading cocatalyst. Chem Lett 2006;35:274–5. https://doi.org/10.1246/CL.2006.274.
[13] Jia Q, Miseki Y, Saito K, Kobayashi H, Kudo A. InBO3 photocatalyst with calcite structure for overall water splitting. Bull Chem Soc Jpn 2010;83:1275–81. https://doi.org/10.1246/BCSJ.20100137.
[14] Wang G, Jing Y, Ju J, Yang D, Yang J, Gao W, et al. Ga4B2O9: an efficient borate photocatalyst for overall water splitting without cocatalyst. Inorg Chem 2015;54:2945–9. https://doi.org/10.1021/IC5031087.
[15] Yu Y, Tang Y, Yuan J, Wu Q, Zheng W, Cao Y. Fabrication of N-TiO2/InBO3 heterostructures with enhanced visible photocatalytic performance. J Phys Chem C 2014;118:13545–51. https://doi.org/10.1021/JP412375Z.
[16] Sharma M, Singhal T, Vaish R. Effect of ferroelectric polarization on piezo/photocatalysis in Ag nanoparticles loaded 0.5(Ba0.7Ca0.3)TiO3–0.5Ba(Zr0.1Ti0.9)O3 composites towards the degradation of organic pollutants. J Am Ceram Soc 2022;105:3165–76. https://doi.org/10.1111/JACE.18298.
[17] Luo F, Qin Y, Shang F, Chen G. Crystallization temperature dependence of structure, electrical and energy storage properties in BaO–Na2O–Nb2O5–Al2O3–B2O3 glass ceramics. Ceram Int 2022. https://doi.org/10.1016/J.CERAMINT.2022.07.011.
[18] Senanon W, Phaiboon P, Chanlek N, Poo-arporn Y, Pinitsoontorn S, Maensiri S, et al. Effect of Mn on lithium-sulphate-borated based glass as energy storage applications. J Non-Cryst Solids 2021;552:120445. https://doi.org/10.1016/J.JNONCRYSOL.2020.120445.
[19] Khajonrit J, Montreeuppathum A, Kidkhunthod P, Chanlek N, Poo-arporn Y, Pinitsoontorn S, et al. New transparent materials for applications as supercapacitors: manganese-lithium-borate glasses. J Alloys Compd 2018;763:199–208. https://doi.org/10.1016/J.JALLCOM.2018.05.300.
[20] Luo F, Xing J, Qin Y, Zhong Y, Shang F, Chen G. Up-conversion luminescence, temperature sensitive and energy storage performance of lead-free transparent Yb3+/Er3+ co-doped Ba2NaNb5O15 glass-ceramics. J Alloys Compd 2022;910:164859. https://doi.org/10.1016/J.JALLCOM.2022.164859.
[21] Feng Y, Ling L, Wang Y, Xu Z, Cao F, Li H, et al. Engineering spherical lead zirconate titanate to explore the essence of piezo-catalysis. Elsevier [n.d].
[22] Kiani A, Nabiyouni G, Masoumi S. A novel magnetic MgFe2O4–MgTiO3 perovskite nanocomposite: rapid photo-degradation of toxic dyes under visible irradiation. Compos B Eng 2019;175:107080.
[23] Razavi FS, Ghanbari D, Salavati-Niasari M. Comparative study on the role of noble metal nanoparticles (Pt and Pd) on the photocatalytic performance of the BaFe 12 O 19/TiO 2 magnetic nanocomposite: green synthesis, characterization, and removal of organic dyes under visible light. Ind Eng Chem Res 2022. https://doi.org/10.1021/ACS.IECR.2C01066.
[24] Razavi F, Ghanbari D, Chemosphere MS-N. Green synthesis of SrFe12O19@ Ag and SrFe12O19@ Au as magnetic plasmonic nanocomposites with high photocatalytic

performance for degradation of organic. Chemosphere 2022;291:132741.
[25] Li S, Zhao Z, Zhao J, Zhang Z, Li X, Zhang J. Recent advances of ferro-, piezo-, and pyroelectric nanomaterials for catalytic applications. Cite This ACS Appl Nano Mater 2020;2020:1063–79. https://doi.org/10.1021/acsanm.0c00039.
[26] Bößl F, Comyn TP, Cowin PI, García-García FR, Tudela I. Piezocatalytic degradation of pollutants in water: importance of catalyst size, poling and excitation mode. Chem Eng J Adv 2021;7. https://doi.org/10.1016/J.CEJA.2021.100133.
[27] Yousefi S, Alshamsi HAOA. Synthesis, characterization and application of Co/Co3O4 nanocomposites as an effective photocatalyst for discoloration of organic dye contaminants in wastewater and antibacterial properties. J Mol Liq 2021;337:116405.
[28] Yousefi S, Amiri O, Sonochemistry MS-N. Control sonochemical parameter to prepare pure Zn0. 35Fe2. 65O4 nanostructures and study their photocatalytic activity. Ultrason Sonochem 2019;58:104619.
[29] Chen Xiaoyue, Guo Yichen, Bian Ruiming, Ji Yinghong, Wang Xinyu, Zhang Xiaoli, Cui Hongzhi, T J. Titanium carbide MXenes coupled with cadmium sulfide nanosheets as two-dimensional/two-dimensional heterostructures for photocatalytic hydrogen. J Colloid Interface Sci 2022;613:644–51.
[30] Singh G, Sharma M, Vaish R. Transparent ferroelectric glass–ceramics for wastewater treatment by piezocatalysis. Commun Mater 2020;1:1–8. https://doi.org/10.1038/s43246-020-00101-2. 11 2020.
[31] Li M, Luan J, Zhang Y, Jiang F, Zhou X. Spectroscopic properties of Er/Yb co-doped glass ceramics containing nanocrystalline Bi2ZnB2O7 for broadband near-infrared emission. Ceram Int 2019;45:18831–7.
[32] Chen L, Zhang W, Wang J, Li X, Li YXH. High piezo/photocatalytic efficiency of Ag/Bi5O7I nanocomposite using mechanical and solar energy for N2 fixation and methyl orange degradation. Green Energy Enviornment 2021.
[33] Rafique M, Jahangir J, Amin BAZ, Bilal Tahir M, Nabi G, Isa Khan M, et al. Investigation of photocatalytic and seed germination effects of TiO2 nanoparticles synthesized by melia azedarach L. Leaf extract. J Inorg Organomet Polym Mater 2019;29:2133–44. https://doi.org/10.1007/S10904-019-01173-5.
[34] Liu J, Zhao W, Wang B, Yan H. Synthesis, characterization and photocatalytic properties of the Y-doped polar borate photocatalysts: Bi2ZnOB2O6: xY3+. Chem Phys Lett 2019;734. https://doi.org/10.1016/J.CPLETT.2019.136707.
[35] Singh G, Sharma M, Materials RV. Transparent ferroelectric glass–ceramics for wastewater treatment by piezocatalysis. Commun Mater 2020;1:1–8.
[36] Wu J, Qin N, Bao D. Effective enhancement of piezocatalytic activity of BaTiO3 nanowires under ultrasonic vibration. Nano Energy 2018;45:44–51. https://doi.org/10.1016/J.NANOEN.2017.12.034.
[37] Wu J, Xu Q, Lin E, Yuan B, Qin N, Thatikonda SK, et al. Insights into the role of ferroelectric polarization in piezocatalysis of nanocrystalline BaTiO3. ACS Appl Mater Interfaces 2018;10. https://doi.org/10.1021/ACSAMI.8B01991/ASSET/IMAGES/LARGE/AM-2018-01991V_0008.JPEG. 17842–9.
[38] Li Y, Diao Y, Wang X, Tian X, Hu Y, Zhang B, et al. Zn4B6O13: efficient borate photocatalyst with fast carrier separation for photodegradation of tetracycline. Inorg Chem 2020;59:13136–43. https://doi.org/10.1021/ACS.INORGCHEM.0C01425/ASSET/IMAGES/LARGE/IC0C01425_0009.JPEG.
[39] Yuan J, Wu Q, Zhang P, Yao J, He T, Cao Y. Synthesis of indium borate and its application in photodegradation of 4-chlorophenol. Environ Sci Technol 2012;46:2330–6. https://doi.org/10.1021/ES203333K/ASSET/IMAGES/LARGE/ES-2011-03333K_0010.JPEG.
[40] Wang K, Han C, Li J, Qiu J, Sunarso J, Liu S. The mechanism of piezocatalysis: energy band theory or screening charge effect? Angew Chem 2022;134. https://doi.org/10.1002/ANGE.202110429.
[41] Ghows N, Entezari MH. Kinetic investigation on sono-degradation of Reactive Black 5 with core–shell nanocrystal. Ultrason Sonochem 2013;20:386–94. https://doi.org/10.1016/J.ULTSONCH.2012.06.013.
[42] Tezcanli-Güyer G, Ince NH. Individual and combined effects of ultrasound, ozone and UV irradiation: a case study with textile dyes. Ultrasonics 2004;42:603–9. https://doi.org/10.1016/J.ULTRAS.2004.01.096.
[43] Tu S, Guo Y, Zhang Y, Hu C, Zhang T, Ma T, et al. Piezocatalysis and piezo-photocatalysis: catalysts classification and modification strategy, reaction mechanism, and practical application. Wiley Online Libr; 2020. p. 30. https://doi.org/10.1002/adfm.202005158.